Characteristics of Premixed Homogeneous Charge Compression Ignition (HCCI) Diesel Combustion and Emissions

Z. Peng , H. Zhao*, and T. Ma

(Department of Mechanical Engineering, Brunel University)

ABSTRACT

This paper reports the outcome from a systematic investigation carried out on HCCI (Homogeneous Charge Compression Ignition) combustion of a diesel type fuel. The n-heptane was chosen in this study to study the premixed diesel HCCI combustion characteristics with port fuel injection. Measurements were carried out in a single-cylinder, 4-stroke and variable compression ratio engine. Premixed n-heptane/air/EGR mixture was introduced into the cylinder by a port fuel injector and an external EGR system. The operating regions with regard to Air/Fuel ratio and EGR rate were established for different compression ratios and intake temperatures. The effects of compression ratios, intake temperatures, Air/Fuel ratios and EGR rates on knock limit, auto-ignition timing, combustion rate, IMEP, and engine-out emissions, such as NOx, CO, and unburned HC, were analysed. The results have shown HCCI combustion of n-heptane could be implemented without intake charge heating with a typical diesel engine compression ratio. The attainable HCCI operating region was mainly limited by the knock limit, misfir, and low IMEP respectively. Higher intake temperature or compression ratio could extend the misfire limit of the HCCI operation at low load but they would reduce the maximum IMEP limit at higher load conditions. Compared with conventional diesel combustion, HCCI combustion lead to extremely low NOx emissions (less than 5 ppm) and smoke free exhaust. But HCCI diesel combustion was found to produce higher HC and CO emissions. An increase in intake temperature or compression ratio helped to reduce HC and CO emissions..

Key words: HCCI, autoignition, diesel engine, EGR, emission

*Corresponding author

1. INTRODUCTION

The superior performance and efficiency of diesel engines, as compared to other types of combustion engines, make them the preferred power plant for heavy-duty vehicles and other commercial applications needs. However, diesel engine designers are currently challenged by the need to comply with ever more stringent emission standards while at the same time with improved engine efficiency. For conventional diesel engines, because soot is formed in the fuel rich regions and NOx in the high temperature regions, it has proved difficult to reduce both NOx and soot simultaneously. To eliminate the problem with fuel rich regions and high temperature regions, HCCI (Homogeneous Charge Compression Ignition) combustion has been proposed and is being intensively investigated by the automotive industry and academics.

HCCI combustion involves the compression-ignition of a premixed combustible charge. It has emerged as a viable alternative combustion process to the conventional spark ignition (SI) or compression ignition (CI) process for internal combustion (IC) engines, owing to its potential for high efficiency and extremely low emissions. Relevant researches on HCCI combustion can be traced back to at least the late 1970's [1-2]. But it was not until the last decade that HCCI combustion has become a topic of intense interest. The initial studies on HCCI combustion were mostly carried out on two-stroke gasoline engines. Since the late 1990's, a number of studies has been reported on HCCI combustion in four-stroke diesel engines. Compared to gasoline engines, HCCI combustion in diesel engines has the potential to achieve simultaneous reduction in both oxides of nitrogen (NOx) and smoke emissions, due to the lack of high temperature and fuel rich zones within the cylinder [3-6].

HCCI diesel combustion has been demonstrated with fully premixed mixture using port-fuel injection and more often with early injection of fuel directly into the cylinder. In the case of premixed HCCI operation, special arrangement was necessary, such as intake charge heating and/or special port fuel injection system, to obtain complete vaporisation of fuel in the intake

system [5-8, 16]. In contrast, the direct injection approach is more compatible with the production engine, whether the early injection [9-12] or late injection [13-15] was used.

Currently, main challenges facing HCCI combustion are the control of the onset of auto-ignition, the rate of heat release, and its limited operational range expanding combustion range. In conventional diesel engines, the start of combustion and its subsequent heat release are controlled indirectly by the fuel injection timing and the rate of fuel injection. But, the ignition timing and heat release rate in a HCCI combustion has to search and adjust suitable charge conditions in order to get ignition timing and combustion engine is affected by a number of engine parameters and hence, difficult to control. A better and thorough understanding of the effects of engine operating parameters on HCCI combustion performance and emissions will be necessary for optimising HCCI combustion. Such results will also be valuable for the advancement of predictive computer models.

In this paper, the results will be presented of premixed HCCI combustion in a four-stroke engine running with a diesel type fuel, n-heptane. In order to concentrate on the autoignition and combustion processes involved, the processes involved in the fuel atomisation, evaporation, and its mixing with air were excluded by means of port fuel injection of a highly volatile fuel, n-heptane that has a similar cetane number to diesel fuel. The HCCI operation regions with regard to air/fuel ratio and EGR were determined for different compression ratios and intake temperatures. The effects of engine operating parameters on the autoignition timing, combustion period, and exhaust emissions will be presented and analysed.

2. EXPERIMENT

2.1 Test Engine

The research engine used for this investigation was a Ricardo E6, which is of the single cylinder type with overhead poppet valves, and has a bore of 76mm and a stroke off 111mm. The combustion chamber is cylindrical in shape. The compression ratio of the engine is continuously

variable between 4.5 and 20, and may be changed during engine operation by means of a worm gear that controls the cylinder head height relative to the crankshaft. The engine is coupled to swinging field AC dynamometer allowing accurate manual speed control. Table 1 summarizes its specifications.

Table 1 Specifications of Ricardo E6 research engine

Intake Valve Opening	10º ATDC
Intake Valve Closing	10º BTDC
Exhaust Valve Opening	10º ATDC
Exhaust Valve Closing	20º BTDC
Bore	76 mm
Stroke	111 mm
Displacement	0.50 litre
Connecting rod length	24.5 cm
Compression ratio	4.5 ~ 20

The test fuel, n-heptane, was delivered to the intake air through a standard Bosch port fuel injector at 2.7 bar. The fuel injection was controlled with the use of purpose built Electronic Control Units. The injection timing was 10º ATDC during intake stroke. The amount of fuel injected varied from 3.5g/cycle to 10g/cycle depending on different operating conditions.

To implement HCCI combustion in the engine, a number of modifications to the intake and fuel system were required. Figure 1 shows the external EGR system used to obtain EGR rates of up to 70-80% (by mass) during testing. EGR was admitted through a gate valve to the inlet manifold approximately 1 meter upstream of the inlet port. This arrangement served two purposes: (i) to allow the EGR/air mixture to become homogeneous before entering the cylinder, and (ii) to cool or reheat the EGR through an EGR cooler or an air heater. This could effectively de-couple the initial charge temperature from the exhaust gas temperature, which would not be the case if exhaust were admitted downstream of the heater.

A 3KW air heater was closed-loop controlled to allow the inlet port temperature held accurately to within $\pm 1^{o}C$. Similarly, the engine coolant temperature was also closed-loop

controlled, set at 80°C ±0.2°C. This was found necessary to ensure that the cylinder head temperature remained constant irrespective of engine load.

2.2 Measurement Systems

Heat release analysis was performed by a computer based data acquisition system. A real-time analysis program has been developed at Brunel University based on the Labview® data acquisition system. The cylinder pressure from a water-cooled pressure transducer (Kistler type 7061B) was recorded by the system from which heat-release data, net-indicated mean effective pressure (IMEP), and coefficient of variation in IMEP (COVimep) were then calculated. Real-time knock analyses could also be carried out by setting a band-pass filter to single out the characteristic engine knock frequency (≈8KHz). Measurements of the amplitude of this filtered trace resulted in very accurate determination of the knock-limited boundary of each operation condition. In this study, an amplitude threshold of 0.5 bar was set to define whether knock had occurred for each individual cycle. Considering the cyclic variations, when measuring incipient and non-destructive knock phenomenon within the engine, a sample number of cycles will contain both knocking cycles and non-knocking cycles. The Knock Occurrence Frequency (KOF) is a measure of the percentage of knocking cycles (knocking above the predefined 0.5 bar threshold) out of the total number of cycles recorded. In this study, the engine is said to be knocking if the KOF equalled or exceeded 10%.

NOx measurements were taken using a SIGNAL 4000VM heated vacuum NOx analyser and unburned Hydrocarbon emissions were measured using a SIGNAL 3000HM FID total hydrocarbon analyser. Both analysers used heated sample lines to minimise errors associated with water condensation and species absorption.

2.3 Test procedure

Preliminary testing was necessary to determine the acceptable engine operating conditions that would allow a reasonable HCCI region for each of the compression ratios and the intake temperatures being tested. Intuitively, the size of the region (A/F ration and EGR rate) should be dependent on the relative difference between the actual end-of-compression charge temperature and the minimum required to auto-ignite the fuel. After some experimentation, the engine conditions giving reasonable HCCI operational range in the study were set at:

Engine Speed	1500rpm
Airflow	WOT
Coolant Temperature	80^{o}C
Oil Temperature	55^{o}C
Inlet Charge Temperature	30^{o}C, 70^{o}C, 105^{o}C
Compression Ratio	12:1, 15:1, 18:1

All of the tests carried out here were performed under the above operating conditions. When the effect of different compression ratios was examined, the intake temperature was fixed at 105^{o}C. The compression ratio was fixed at 18:1 when the effect of different intake temperatures was tested. To obtain enough coolant and oil temperature, it was necessary to run the engine through a warm-up procedure for 1 hour. All the testing was carried out at wide open throttle (WOT) and the A/F ratio was by varied by the fuel flow rate through the injector. EGR rate was gradually increased in increments of approximately 10% for each fuel setting, from zero to maximum allowable for combustion to occur. For every operating condition, the result was averaged over 100 cycles.

2.4 Determination of Lambda and EGR Rate

For each experimental condition, the engine was operated at a constant compression ratio, intake temperature, fuel flow rate and EGR valve opening. In-cylinder relative air/fuel ration, Lambda, and EGR rate were calculated by measuring dry molar fractions of O_2, CO_2 and CO in the inlet and the exhaust lines by an OLIVER K650 MOT analyser (see Figure 1).

An analytical approach has been developed for calculating the overall A/F ratio and EGR rate in the cylinder. A set of equations relating inlet and exhaust gas species including CO and unburned HC allows the simultaneous calculation of A/F ratio and EGR rate without measuring inlet airflow directly. This has advantages over less accurate methods (e.g. UEGO sensors) that do not account for exhaust unburned hydrocarbons, which can be a significant proportion of the injected fuel under some HCCI combustion conditions. The calculation is mainly based on the combustion equation:

$$n_R[aCH_bO_c + d(O_2 + 3.773N_2)] = (n_P - n_R f)(g_e CO_2 + h_e CO + j_e O_2 + k_e N_2 + l_e H_2O + s_e CH_4)$$

(1)

Where, N_R and N_P are the number of moles of reactants and products respectively. a and d are wet molar fraction of injected fuel and inlet air (not including excess air in EGR) respectively. g_e, h_e, j_e, k_e, l_e and s_e are wet molar fraction of their following species in exhaust gas respectively.

In equation (1), H_2 in the exhaust gas is omitted as the engine was always operated with lean air/fuel mixtures. NOx emissions are also negligible. The wet molar fractions of O_2, CO_2 and CO in inlet gas and exhaust gas are related to the measured dry molar fractions by

$$x = (1 - l)x'$$

(2)

And the wet molar fraction of exhaust products in the inlet mixture including excess air is

$$f = \frac{x_i}{x_e} \Rightarrow x_i = f \cdot x_e$$

(3)

By solving the following carbon balance equation, oxygen balance equation and hydrogen balance equation

$$n_R a = (n_P - n_R f)(g_e + h_e + s_e)$$

(4)

$$n_R (ac + 2d) = (n_P - n_R f)(2g_e + h_e + 2j_e + l_e)$$

(5)

$$n_R ab = (n_P - n_R f)(2l_e + 4s_e)$$

(6)

The in-cylinder air/fuel ratio is given by

$$A/F \;\; Ratio = \frac{\dot{m}_a}{\dot{m}_f} = \frac{n_R (c + g_i)(32 + 3.773 * 28.16)}{n_R [a(12.011 + 1.008b + 16c) + fs_e (12.011 + 4 * 1.008)]}$$

(7)

and the gravimetric EGR rate is given by

$$EGR_m = \frac{\dot{m}_{EGR}}{\dot{m}_{EGR} + \dot{m}_r}$$

(8)

Where b and c are the H/C ratio and O/C ratio of fuel, respectively. m_a, m_f, m_{EGR} and m_r are the masses of air, fuel, EGR and reactant components (intake air and injected fuel) respectively.

2.5 HCCI Combustion Analasis

In HCCI combustion, heat release at any instant involves the burning of all the fuels in the cylinder. Therefore the concept of the fraction of heat released is introduced, in a similar way to that of the mass fraction burned in the analysis of premixed spark ignition combustion. Figure 2 shows such a heat fraction released curve for n-heptane. It can be seen that the curve is characterised by a two-stage auto-ignition and heat release process. As it was shown by Halstead et al [17], the first stage of the autoignition and heat release is associated with the cool flame or the low temperature reactions following the partial oxidation of fuel molecule and its subsequent

isomerisation. The second stage 'hot' ignition is caused by the formation of more active branching agent at the higher temperature following the low temperature reactions. Figure 2 shows that the amount of heat released during the first stage was less than 20% in most cases and it varied with the Air/Fuel ratio and the amount of EGR. The higher the EGR rate, the less heat released in the first stage. In contrast, the leaner the mixture the more heat released in this stage.

Since the period between the two stages could be as long as 15 CA, it was necessary to determine the auto-ignition timings of both the first stage and the second stage involved in the heat release process as shown in Figure 3. In addition, the start and the end of the combustion was considered to occur at the crank angles when the rate of heat fraction released had increased to above or decreased to below 1 %/CA degree. Therefore, the combustion duration was defined as the period during which the the rate of heat fraction released was greater than 1 % /CA.

3. RESULTS AND DISCUSSION

After some preliminary testing, the following engine experiments were carried out. The first series of experiments were performed at a constant compression ratio of 18:1, typical of a direct injection diesel engine, with three different intake temperatures at 30^{o}C, 70^{o}C and 105^{o}C. The second series of experiments were done under three different compression ratios of 18:1, 15:1 and 12:1 at a constant intake temperature of 105^{o}C, so that the effect of compression ratio could be investigated.

3.1 HCCI Operational Region

Figure 4 shows the engine's HCCI operation region when it was operated at 18:1 compression ratio and 30ºC intake temperature. The horizontal axis represents the total gravimetric percentage of EGR in the cylinder, and the vertical axis represents the overall relative Air/Fuel ratio (Lambda or λ) of the cylinder charge. The figure shows that diesel HCCI combustion could be achieved over a very wide range of A/F ratios and EGR rates at a compression ratio of 18:1. The bottom (high load) limit of the HCCI region was bounded by the knocking combustion or the rapid heat

release rate as the mixture became richer. Unlike the gasoline HCCI opeation in the same engine [18], the knock limit of the HCCI combustion of n-heptane could not be operated near Lambda 1.0. This was true even at lower compression ratios and higher intake temperatures, as to be shown later. In addition, the Lambda attainable at zero EGR was approximately 5.0~6.0, much higher than the Lambda 3.0 as observed with gasoline HCCI combustion [18]. Furthermore, the n-heptane HCCI combustion could tolerate a very high EGR rate of up to 80%.

The right and the top-right of the region was limited by misfire due to the increasing amount of CO_2 and H_2O at higher EGR rates. When operating near this limit, the engine operation was characterised with intermittent misfire cycles. The frequency of misfire increased as the limit was approached. This could be explained by the fact that a misfire cycle led to a reduction in CO_2 and H_2O in the cylinder charge in the following cycle and hence, effectively shifted the operating point from right to top left (low EGR, high λ). After several misfire cycles, the in-cylinder condition would be such that stable HCCI combustion could start again until CO_2 and H_2O content in exhaust gases would extinguish the combustion again. This is shown as increased COVimep in Figure 5. However, it should be pointed out that at the top left region, the engine operation was stable untill the IMEP reached zero, despite the high COVimep values shown in Figure 5. The increase of COVimep at this area was probably caused by the small IMEP values. Therefore, the top left limit of diesel HCCI combustion was actually determined by the lower limit of IMEP that would be sufficient to overcome the frictional losses in the engine.

Figure 4 also shown the engine's output was controlled by the air/fuel ratio as the amount of fuel injected was reduced as shown in Figure 6. There was a maximum IMEP (4 bar) triangle area around Lambda 1.5 and EGR rate 65%. It is noted that the IMEP value in this area was very sensitive to the EGR rate. A slight increase in EGR rate could cause the engine to misfire, as indicated by the large COVimep variation in Figure 5.

3.2 Effect of Compression Ratio and Charge Temperature on HCCI Operational Region

The effect of the intake temperature on the HCCI operation was investigated at 30°C, 70°C and 105°C with a constant compression ratio 18:1 and the results are shown in Figure 7. As the intake charge temperature was increased from 30°C to 105°C, the top (lean) and bottom (rich) limits were hardly affected. However, the higher intake charge temperature did substantially extend the misfire limit to much higher EGR rate. In the present engine setup, the maximum EGR rate was limited to 80% due to limited backpressure available.

Figure 8 shows the effect of the intake temperature for two EGR rates. Lines with solid symbols represent the results without EGR and lines with empty symbols are with 40% EGR rate. It can be seen, regardless of the EGR rate, a lower intake temperature produced a higher IMEP value and this trend was more noticeable at lower Air/Fuel ratios. The maximum IMEP was reduced from 3.7vbar to 2.7vbar as the intake temperature was increased from 30°C to 105°C. This was mainly due to the reduction of the in-cylinder charge mass with the increase in intake temperature.

The effect of the compression ratio was examined at 18:1, 15:1 and 12:1 with a constant intake temperature of 105°C and the results are shown in Figure 9. It can be seen that higher compression ratio extended substantially both the misfire limit at high EGR and low load limit at high λ. However, the increase in compression ratio reduced the knock limit and caused the maximum IMEP to drop from 3.5 bar to 2.7 bar. Figure 10 shows the effect of compression ratio on IMEP at two EGR rates. It is noted that, with a relatively rich (small λ) mixture without EGR, higher CR produced lower IMEP for same Lambda value and intake temperature. This may appear contradictory to the conventional thinking or experience that high compression ratio should lead to higher engine output. Close examination of their ignition timings and combustion durations from the heat release analysis, it was found that higher CR resulted in a very early autoignition timing and a very short combustion duration (this will be shown in the next section) for a relatively rich mixture without EGR. As a result, the combustion took place during the end

of the compression stroke and hence, reduced power output. However, under high dilution conditions such as high Air/Fuel ratio or high EGR rate, higher CR led to higher IMEP value.

If regarding CR 18:1 and intake temperature 105^{o}C as a baseline, according to Figure 7 and Figure 8, the higher load limit of a diesel engine's HCCI operation can be increased by either or both lower intake temperature and compression ratio. In practice, the lower intake temperature can be readily facilitated with a combination of a intercooler and EGR cooler. Whereas, the variable compression ratio will require a much more sophisticated engine design or/and flexible valve actuation system.

3.3 Effect of the A/F ratio and EGR on Autoignition Timing and Combustion Duration

Figure 11 and Figure 12 shows the autoignition timing contours of the low temperature reaction (LTR) and its duration with 18:1 CR and 30^{o}C T_{in}. As described in section 2.5, the start and end of LTR is defined as the crank angle at which the rate of HFR was above 1 %/(CA degree). It can be seen that the LTR auto-ignition timing was affected dominantly by the EGR rates. It is known that EGR can affect the autoignition process through its dilution effect (replacement of O_2) and heat capacity effect (lower compression temperature). Since the mixture was very lean with abundant oxygen and the fact that the A/F ratio had little effect on the mixture's LTR autoignition timing, the lower compression temperature due to EGR's higher heat capcity was likely responsible for the retarded start of LRT. In contrast, Figure 12 shows that the LTR duration was affected only by the A/F ratio. The results indicate that the low temperature reactions took place over a longer period of time as the mixture became leaner.

Figure 13 shows the effect of A/F and EGR rate on the start of the main combustion stage (MCS). Here 'start' rather than 'autoignition timing' is used because autoignition has already started from the low temperature reactions stage. The start of MCS is critical for the total combustion process as most heat is released during the main combustion stage. If the complete

combustion process is considered in its entirety, this timing should be treated as its autoignition timing. As shown in Figure 13, the start of the main combustion stage was affected by both the A/F ratio and EGR rate. For very lean mixtures (λ>9.0), it was mainly dependent upon the A/F ratio. For other mixtures, the EGR rate had a dominant effect on the start of MCS.

As shown in Figure 14, the combustion duration of the main combustion stage was affected by the A/F ratio in most of the HCCI operational region, other than the maximum IMEP triangular area with the richest mixture and higher EGR rate. In the region where the effect of the A/F ratio dominated, the combustion duration was longest in the middle part of the map. This could be caused by the combined effect of slower reactions and smaller quantities of fuels to be burned. Initially, as the mixture became leaner the combustion reactions slowed down due to lower combustion temperature. As the mixture became even leaner, the reduction in the amount of fuel to be burned dropped substantially that the overall combustion duration started to decrease.

3.4 Effect of Charge Temperature and Compression Ratio on Autoignition Timing and Combustion Duration

Figure 15 and Figure 16 show effects of the intake temperature (T_{in}) and the compression ratio (CR) on the LTR autoignition timing. It can be seen that the higher T_{in} or CR, the earlier the LTR started, as the end-of-compression charge temperature was raised with increasing T_{in} or CR. For every 35-40ºC increase in T_{in} or 3 unit increase in CR, the autoignition timing of low temperature reactions advanced by 4-5 CAs, irrespective of the A/F ratio and EGR rate. The effects of CR and T_{in} on the combustion duration of LTR are shown in Figure 17 and Figure 18. As expected, either higher T_{in} or higher CR reduced in the LTR combustion duration.

Figure 19 and Figure 20 shows the effect of the intake temperature and compression ratio on the start of the main combustion stage. When the intake temperature was increased from 30°C to 70°C, the start of main combustion was brought forward by 3-4 CAs, independent of the A/F ratio or EGR. Further increase in temperature from 70°C to 105°C had less effect on the main combustion timing. In addition, it is noted from Figure 15 and Figure 19 that the charge

temperature had less impact on the start of the main combustion than that of the low temperature reactions, particularly in the high EGR region. As shown in Figure 20, for every 3 unit increase in the compression ratio, the main combustion was advanced by about 5-6 CAs, similar to its effect on the autoignition timing of the low temperature reactions.

Figure 21 and Figure 22 shows the effect of the intake temperature and compression ratio on the main combustion duration. For relatively rich mixtures, the combustion period was reduced as the intake temperature went up. The shorter combustion duration observed for very lean mixtures was due to the onset of partial burning. In addition, the results show that the effect of the intake temperature on the combustion duration was more noticeable with EGR than without EGR. As shown in Figure 22, the compression ratio had a similar but large effect on the main combustion duration, due to both increased temperature and pressure.

3.5 Exhaust Emissions

Figure 23 shows the effect of A/F and EGR rate on NOx emissions (ppm) at 18:1 CR and 30 ^{o}C intake tempeature. From the map, it can be seen that NOx emissions were very low. This can be readily explained by the results shown in Figure 24, in which the maximum combustion temperature contours calculated from in-cylinder pressure data were plotted. As the combustion temperature was well below the critical temperature of 1800K for NO formation, little NO was produced during the HCCI combustion operation.

HC emissions (ppm) map with regard to Air/Fuel ratio and EGR rate is shown in Figure 24. The highest HC emission occurred on the right hand side of the HCCI region, where misfire started to appear. The minimum HC formation was located at Lambda 9.0 with 10% EGR. The increase in HC emission with leaner mixtures was known to be caused by the lower combustion temperature. However, it is not clear why HC emission increased as the mixture became richer than Lambda 9.0. As shown in Figure 25, CO emissions tend to increase with the A/F ratios and EGR rate. There is little resemblance between the CO and HC contours, despite the fact that both

were result of low temperature combustion. Detailed explanations will require detailed chemical kinetics analyses.

Figure 26 and Figure 27 show effects of the intake temperature and the compression ratio on the HC emissions. In general, increases of intake temperature and compression ratio help reducing the HC emission. Similar effects of the intake temperature and the compression ratio were also observed on the CO emissions, as shown in Figure 28 and Figure 29. The exception was found when the engine was operating at 12:1 compression ratio and high Lambda values, where the sudden increase of HC did not appear in CO emissions.

3.6 Indicated Specific Fuel Consumption (ISFC)

Figure 30 shows the ISFC map of diesel HCCI combustion at a compression ratio of 18:1 and intake temperature 30^{o}C. The lowest ISFC value was about 180g/kw.h. The lowest ISFC was obtained in the richest mixture region, where the maximum IMEP was found. The ISFC increased monotonically with the A/F ratio, probably due to the slower combustion process (see Figure 12).

As shown in Figure 31 and Figure 32, both higher intake charge temperature and higher compression ratio tended to increase fuel consumption. Referring to Figures 19 to 22 and discussion in Section 3.4, the negative effect of charge temperature and compression ratio was probably caused by the advanced combustion phasing in the compression stroke.

4. SUMMARY

Experiments on a single-cylinder, 4-stroke and variable compression ratio engine have been carried out in order to study the Homogeneous Charge Compression Ignition (HCCI) or Controlled Auto Ignition (CAI) combustion of a diesel type fuel. The effects of Air/Fuel ratio, EGR rate, compression ratio and different intake temperature on the HCCI operational region and engine's performance and emissions were investigated. Main findings from the results obtained can be summarised as follows.

1. In the premixed HCCI operation, the autoignition combustion was characterised by the two-stage heat release process. Most heat was released during the second stage of combustion.
2. HCCI diesel engine-out emissions were free from smoke and NOx.
3. Compared to Gasoline HCCI/CAI operation, premixed diesel HCCI combustion could be obtained for a range of A/F ratios and EGR dilutions without intake charge heating. Its operational region was found to be limited at high load by violent combustion with relatively rich mixture, misfire at high EGR dilution, and IMEP output with very lean mixture.
4. The high load limit of HCCI can be extended by operating at a lower compression ratio, and in particular by lowering the intake charge temperature when the violent combustion was caused by the advanced heat release.
5. Both the autoignition timing of the low temperature reactions and the start of the main combustion process were mainly affected by EGR and they were retarded with increasing EGR. Whereas both the low temperature and high temperature combustion durations were mostly dependent upon the A/F ratio.
6. Both increases in the intake charge temperature and compression ratio led to reductions in HC and CO emission. However, the higher charge temperature and higher compression tended to increase the fuel consumption.

ACKNOWLEDGEMENTS

The authors would like to acknowledge the financial support to the work reported here by European Union through the project of SPACE-LIGHT.

REFERENCES

1. Onishi, S., Hong, J. S., Shoda, K., Do, J. P. and Kato, S., Active Thermo-Atmosphere Combustion (ATAC) – A New Combustion Process for Internal Combustion Engines, SAE Paper 790501, 1979.
2. Noguchi, M., Tannka, Y., Tanaka, T. and Takeuchi, Y., A Study on Gasoline Engine Combustion by Observation of Intermediate Reactive Products during Combustion, SAE paper 780840, 1979.
3. Gatellier, B., Walter, B. and Miche, M., New Diesel Combustion Process to Achieve Near Zearo Nox and Particulates Emission, *A New Generation of Engine Combustion Processes for the Future?* Proceeding of the International Congress held in Rueil-Malmaison, France, November, 26-27, 2001, P43.
4. Suzuki, H., Koike, N. and Odaka, M., Combustion Control Method of Homogeneous Charge Diesel Engines, SAE paper 980509, 1998.
5. Ryan, T. W. and Callahan, T. J., Homogeneous Charge Compression Ignition of Diesel Fuel, SAE paper 961160, 1996.
6. Gray, A. W. and Ryan, T. W., Homogeneous Charge Compression Ignition (HCCI) of Diesel Fuel, SAE paper 971676, 1997.
7. Christensen, M., Hultqvist, A. and Johansson, B., Demonstrating the Multi Fuel Capability of a Homogeneous Charge Compression Ignition Engine with Variable Compression Ratio, SAE paper 1999-01-3679, 1999.
8. Siewert, R. M., Homogeneous-Charge Compression-Ignition (HCCI) of Gasoline-Like Fuels in a Single-Cylinder Diesel Engine, *A New Generation of Engine Combustion Processes for the Future?* Proceeding of the International Congress held in Rueil-Malmaison, France, November, 26-27, 2001, P7.
9. Takeda, Y. and Keiichi, N., Emission Characteristics of Premixed Lean Diesel Combustion with Extremely Early Staged Fuel Injection, SAE paper 961163, 1996.

10. Harada, A., Shimazaki, N., Sasaki, S., Miyamoto, T., Akagawa, H. and Tsujimura, K., The Effects of Mixture Formation on Premixed Lean Diesel Combustion. SAE paper 980533, 1998.
11. Akagawa, H., Miyamoto, T., Harada, A., Sasaki, S., Shimazaki, N., Hashizume, T. and Tsujimura, K., Approaches to Solve Problems of the Premixed Lean Diesel Combustion. SAE paper 1999-01-0183, 1999.
12. Iwabuchi, Y., Kawai, K., Shoji, T. and Takeda, Y., Trial of New Concept Diesel Combustion System - Premixed Compression-Ignited Combustion, SAE paper 1999-01-0185, 1999.
13. Krieger, R. B., Siewert, R. M., Pinson, J. A., Gallopoulos, N. E., Hilden, D. L., Monroe, D. R., Rask, R. B., Solomon, A. S. P. and Zima, P., Diesel Engines: One Option to Power Future Personal Transportation Vehicles, SAE paper 972683, 1997.
14. Kimura, W., Aoki, O., Ogawa, H., Muranaka, S. and Enomoto, Y., New Combustion Concept for Ultra-Clean and High-Efficiency Small DI Diesel Engines, SAE paper 1999-01-3681, 1999.
15. Kimura, W., Aoki, O., Kitahara, Y. and Aiyoshizawa, E., Ultra-Clean Combustion Technology Combining a Low-Temperature and Premixed Combustion Concept for Meeting Future Emission Standards, SAE paper 2001-01-0200, 2001.
16. Thring, R. H., Homogeneous-Charge Compression Ignition (HCCI) Engine, SAE paper 892068, 1989.
17. Halstead, M. P., Kirsch, L. J. and Quinn, C. P., The Autoignition of Hydrocarbon Fuels at High Temperature and Pressure-Fitting of a Mathematical Model, Combustion and Flame, vol.30 , p45, 1977.
18. Oakley, A., Zhao, H., Ladommatos, N. and Ma, T., Experimental Studies on Controlled Auto-Ignition (CAI) Combustion in a 4-Stroke Gasoline Engine, SAE paper 2001-01-1030, 2001.

List of notation

AC	alternative current
ATDC	after the top dead centre
A/F	air/fuel ratio
BTDC	before the top dead centre
CA	crank angle
CAI	controlled auto-ignition
CI	compression ignition
CO	carbon monoxide
COV	coefficient of variation
CR	compression ratio
EGR	exhaust gas recirculation
HC	hydrocarbon
HCCI	homogeneous charge compression ignition
IC	internal combustion
IMEP	indicated mean effective pressure
ISFC	indicated specific fuel consumption
IVC	inlet valve closure
KOF	knock occurrence frequency
Lambda	relative air/fuel ratio (λ)
LIF	laser induced fluorescence
LTRS	low temperature reactions stage
MCS	main combustion stage
NOx	nitrogen oxides
NTC	negative temperature coefficient

SI	spark ignition
TDC	top dead centre
T_{in}	intake temperature
uHC	unburnt hydrocarbon

superscript

o	crank angle or temperature
‘	dry molar fraction

subscript

a	air
e	exhaust gas
f	fuel
i	inlet gas
in	inlet gas
P	products
R	reactants

List of figure captions

Fig.17 The effect of Air/Fuel ratio and EGR rate on the start of the main combustion stage. (CR=18:1, T_{in}=105°C)

Fig.18 The effect of the intake temperature on the start of the main combustion stage. (CR=18:1)

Fig.19 The effect of the compression ratio on the start of the main combustion stage. (T_{in}=105°C)

Fig.20 The effect of Air/Fuel ratio and EGR rate on the combustion duration of the main combustion stage. (CR=18:1, T_{in}=105°C)

Fig.21 The effect of the intake temperature on the combustion duration of the main combustion stage. (CR=18:1)

Fig.22 The effect of the compression ratio on the combustion duration of the main combustion stage. (T_{in}=105°C)

Fig.23 The effect of the intake temperature on NOx emissions. (CR=18:1)

Fig.24 The effect of Air/Fuel ratio and EGR rate on NOx emissions. (CR=18:1, T_{in}=105°C)

Fig.25 The effect of Air/Fuel ratio and EGR rate on HC emissions. (CR=18:1, T_{in}=105°C)

Fig.26 The effect of the intake temperature on HC emissions. (CR=18:1)

Fig.27 The effect of the compression ratio on HC emissions. (T_{in}=105°C)

Fig.28 The effect of Air/Fuel ratio and EGR rate on CO emissions. (CR=18:1, T_{in}=105°C)

Fig.29 The effect of the intake temperature on CO emissions. (CR=18:1)

Fig.30 The effect of the compression ratio on CO emissions. (T_{in}=105°C)

Fig.31 The effect of Air/Fuel ratio and EGR rate on ISFC. (CR=18:1, T_{in}=105°C)

Fig.32 The effect of the intake temperature on ISFC. (CR=18:1)

Fig.33 The effect of the compression ratio on ISFC. (T_{in}=105°C)

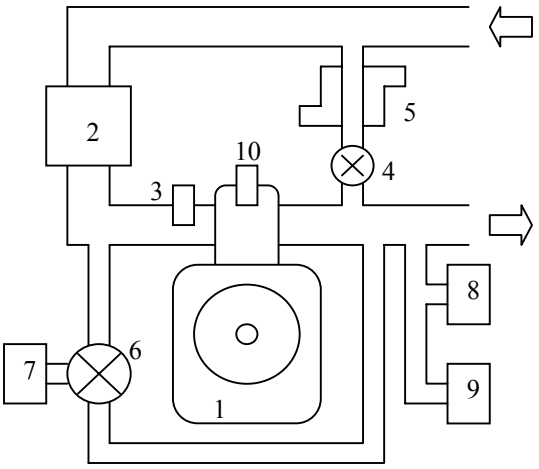

1) Ricardo E6 Engine. 2) Air Heater. 3) Port Injector. 4) EGR Control Valve. 5) EGR Cooler. 6) Intake/Exhaust Sampling Switch. 7) Oliver K750 Exhaust Analyser. 8) HC Analyser. 9) NOx Analyser. 10) Pressure Sensor.

Figure 1 External EGR and gas sampling systems

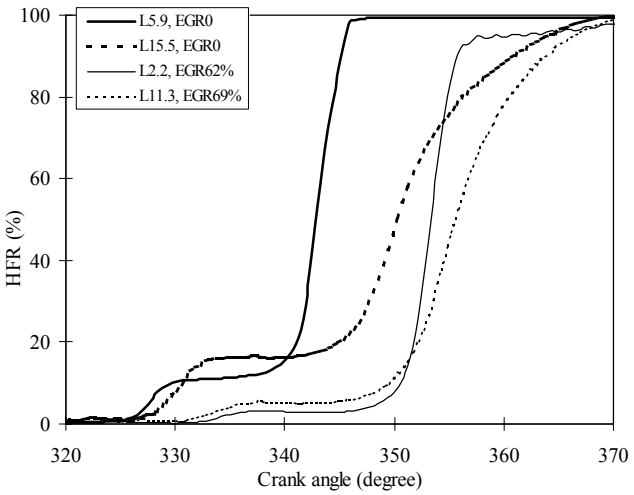

Figure 2 Heat Fraction Released (HFR) curves for different Air/Fuel ratio and EGR rate. (CR=18:1, T_{in}=105°C)

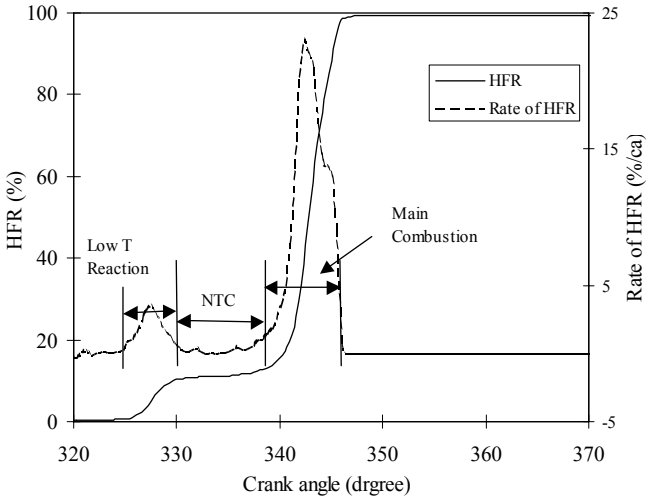

Figure 3 Heat Fraction Released (HFR) and the rate of HFR. (Lambda=5.9, EGR rate=0, CR=18:1, T_{in}=105°C)

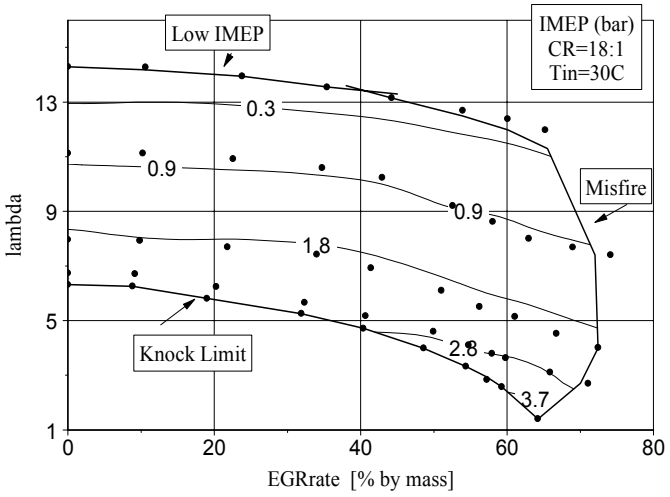

Figure 4 HCCI operating region with regard to Air/Fuel ratio and EGR rate. (CR=18:1 T_{in}=30°C)

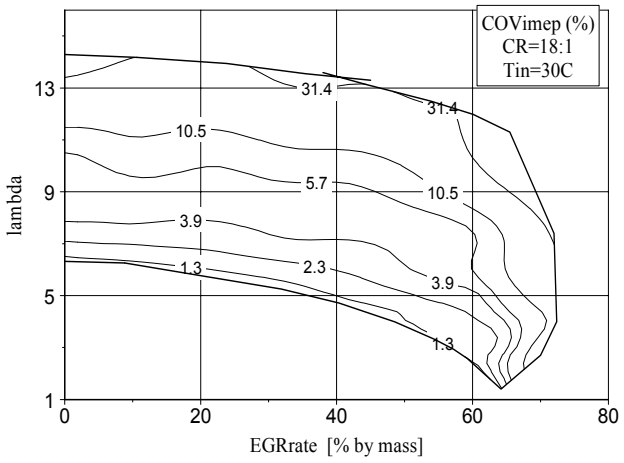

Figure 5 The effect of Air/Fuel ratio and EGR rate on COVimep. (CR=18:1 T_{in}=30°C)

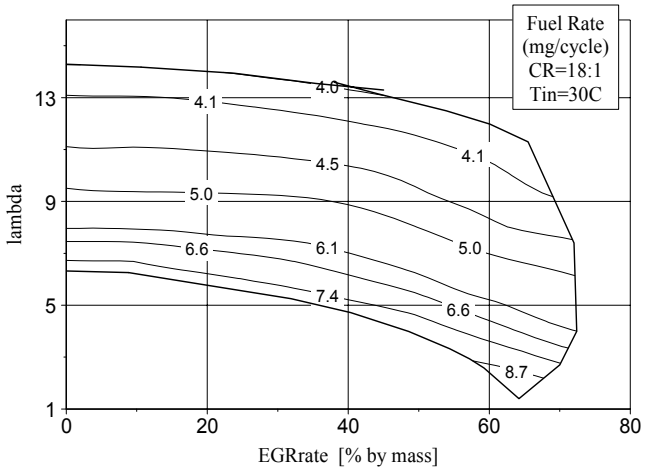

Figure 6. Average fuel mass per cycle (mg/cycle). (CR=18:1 T_{in}=30°C)

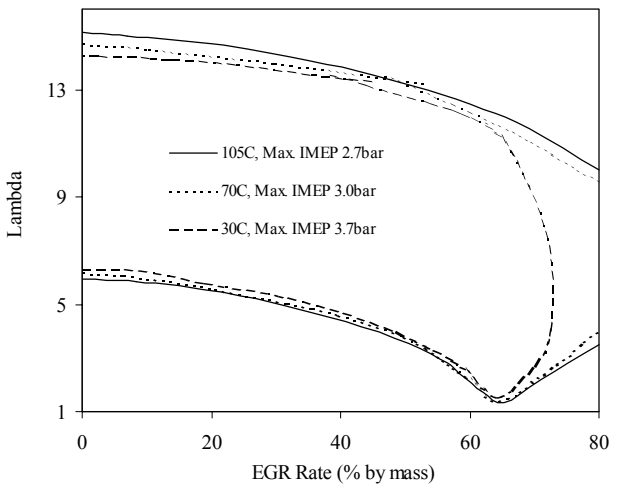

Figure 7 Effect of the intake temperature on HCCI combustion operating region. (CR=18:1)

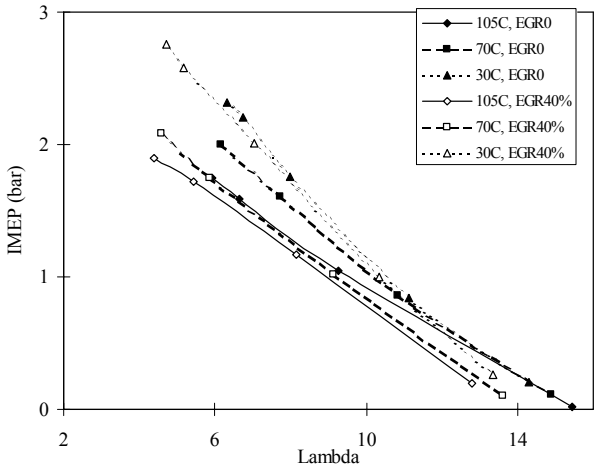

Figure 8 Effect of the intake temperatures on IMEP. (CR=18:1)

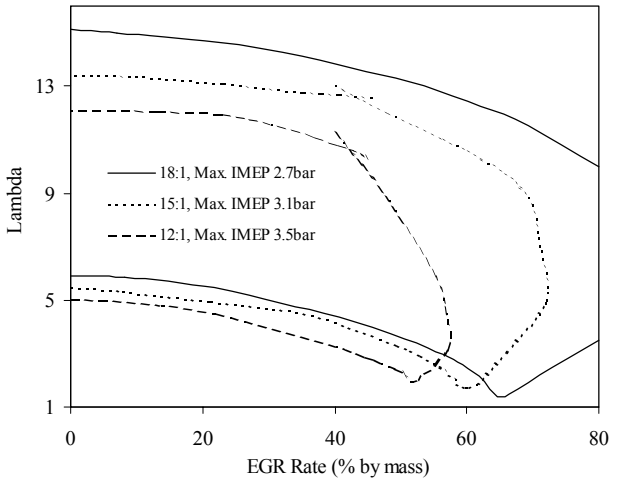

Figure 9 Effect of the compression ratio on HCCI combustion operating region. (T_{in}=105°C)

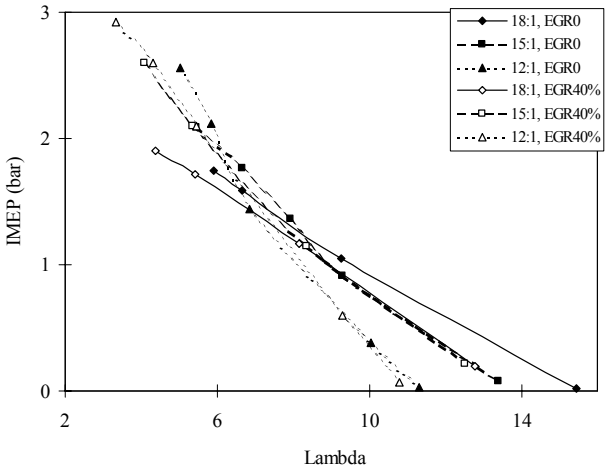

Figure 10 Effect of the compression ratios on IMEP. (T_{in}=105°C)

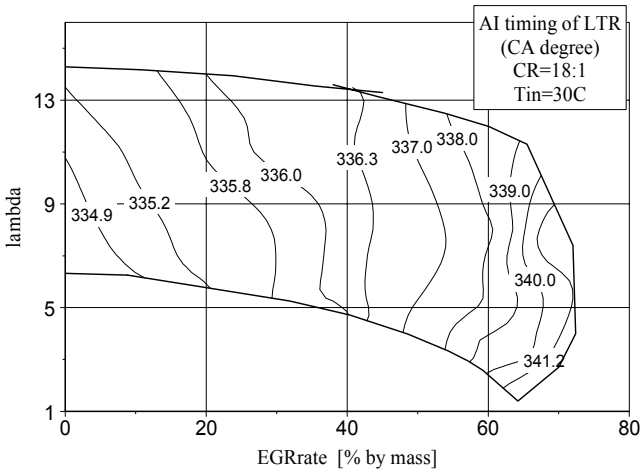

Figure 11 Effect of Air/Fuel ratio and EGR rate on the autoigntion timing of the low temperature reactions stage. (CR=18:1 T_{in}=30°C)

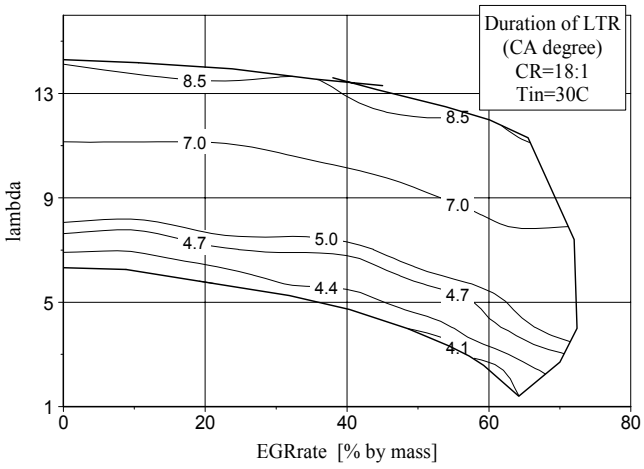

Figure 12 Effect of Air/Fuel ratio and EGR rate on the combustion duration of the low temperature reactions stage. (CR=18:1 T_{in}=30°C)

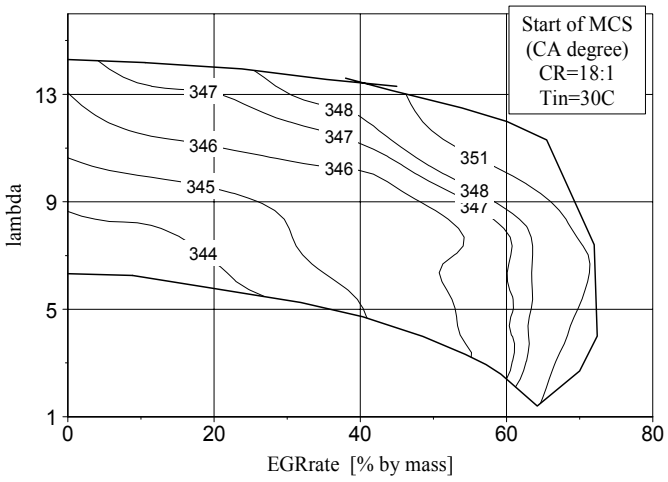

Figure 13 Effect of Air/Fuel ratio and EGR rate on the start of the main combustion stage. (CR=18:1 T_{in}=30°C)

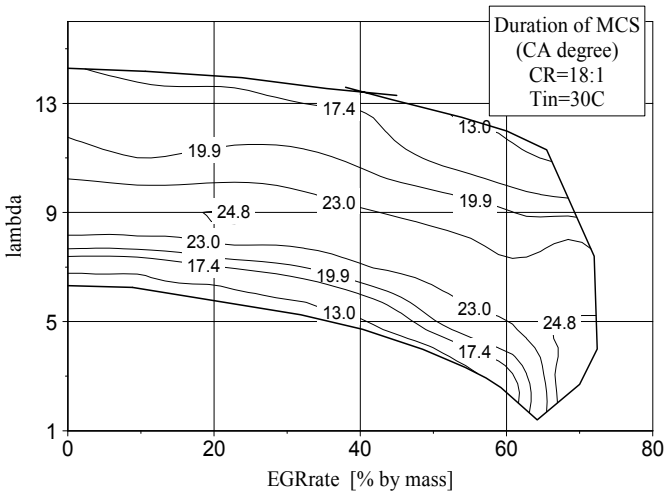

Figure 14 Effect of Air/Fuel ratio and EGR rate on the combustion duration of the main combustion stage. (CR=18:1 T_{in}=30°C)

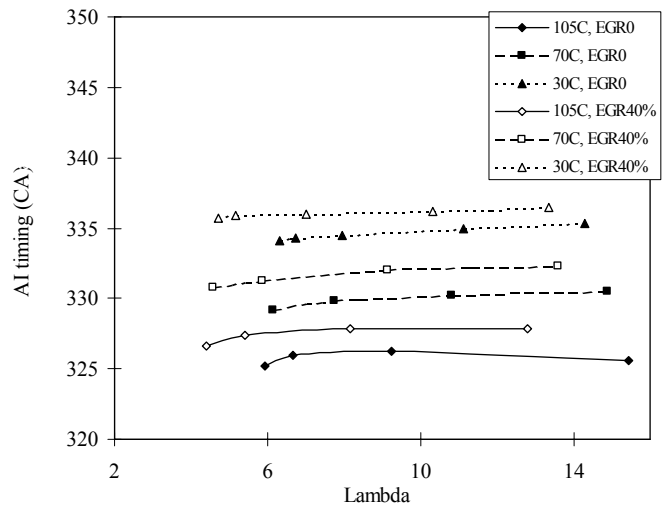

Figure 15 Effect of the intake temperature on the autoignition timing of the low temperature reactions stage. (CR=18:1)

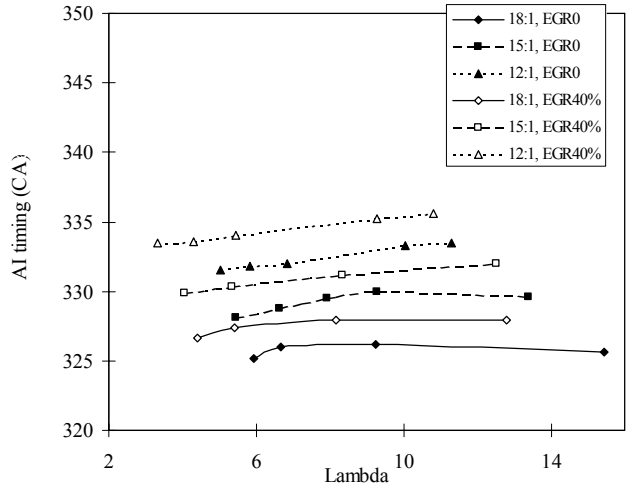

Figure 16 Effect of the compression ratio on the autoignition timing of the low temperature reactions stage. (T_{in}=105°C)

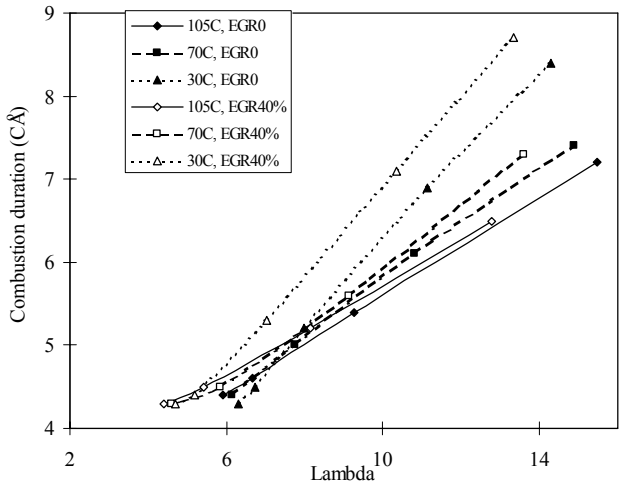

Figure 17 Effect of the intake temperature on the combustion duration of the low temperature reactions stage. (CR=18:1)

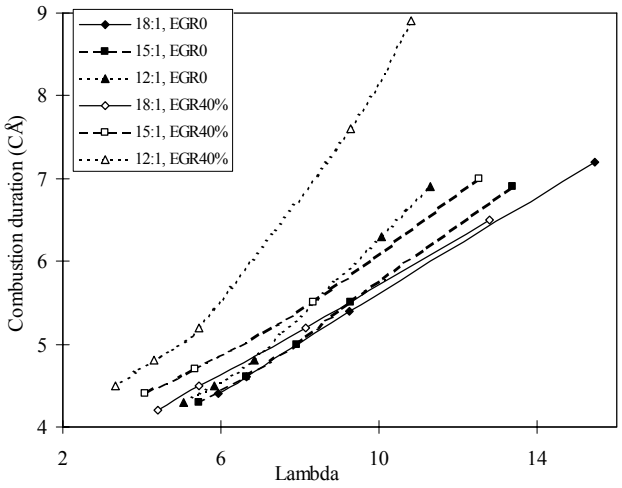

Figure 18 Effect of the compression ratio on the combustion duration of the low temperature reactions stage. (T_{in}=105°C))

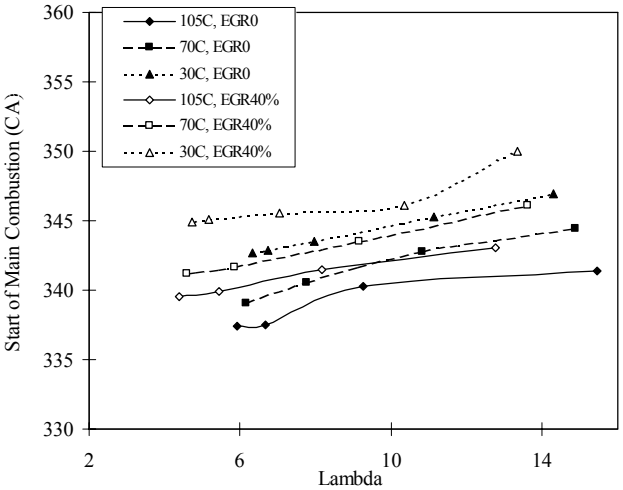

Figure 19 Effect of the intake temperature on the start of the main combustion stage. (CR=18:1)

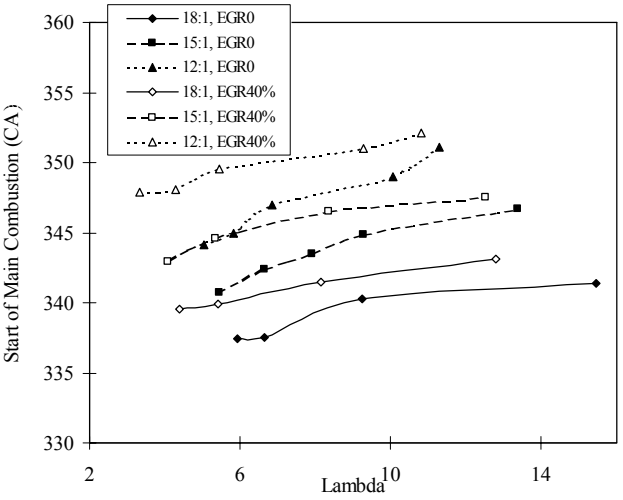

Figure 20 Effect of the compression ratio on the start of the main combustion stage. (T_{in}=105°C)

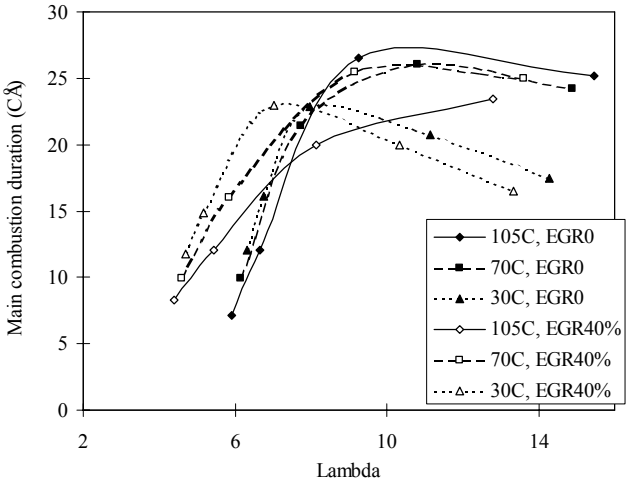

Figure 21 Effect of the intake temperature on the main combustion duration. (CR=18:1)

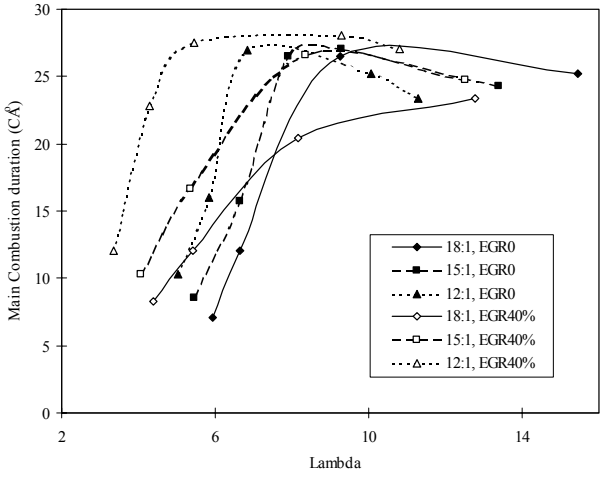

Figure 22 Effect of the compression ratio on the main combustion duration. (T_{in}=105°C)

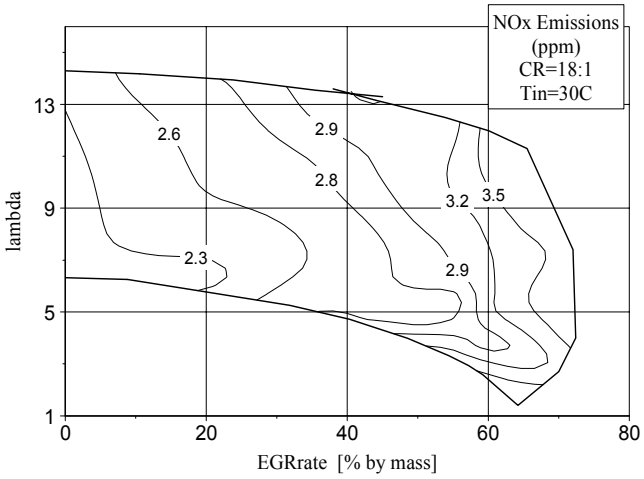

Figure 23 Effect of Air/Fuel ratio and EGR rate on NOx emissions. (CR=18:1 T_{in}=30°C)

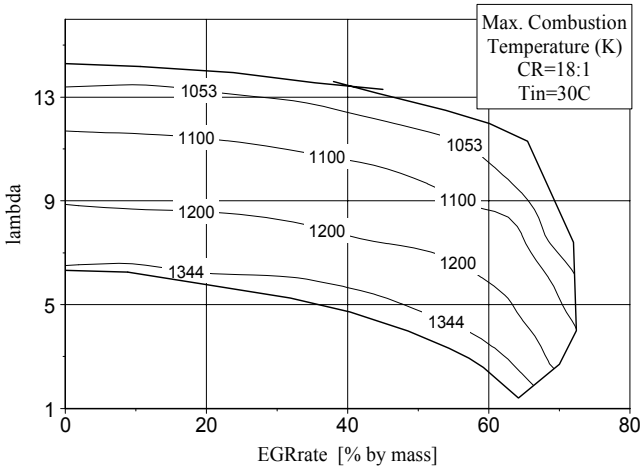

Figure 24 Effect of Air/Fuel ratio and EGR rate on the maximum combustion temperature. (CR=18:1 T_{in}=30°C)

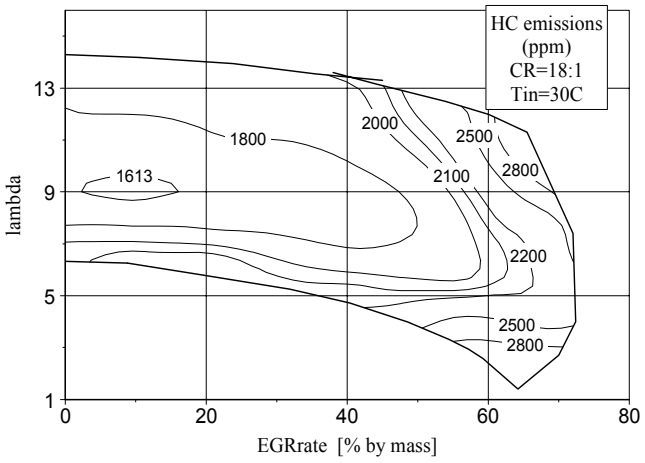

Figure 25 Effect of Air/Fuel ratio and EGR rate on HC emissions. (CR=18:1 T_{in}=30°C)

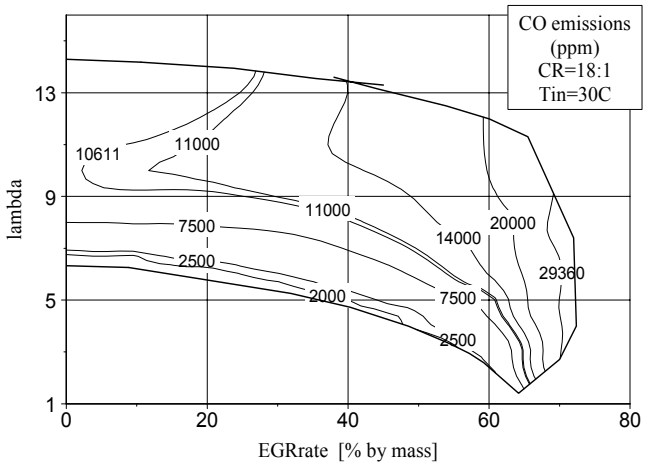

Figure 26 Effect of Air/Fuel ratio and EGR rate on CO emissions. (CR=18:1 T_{in}=30°C)

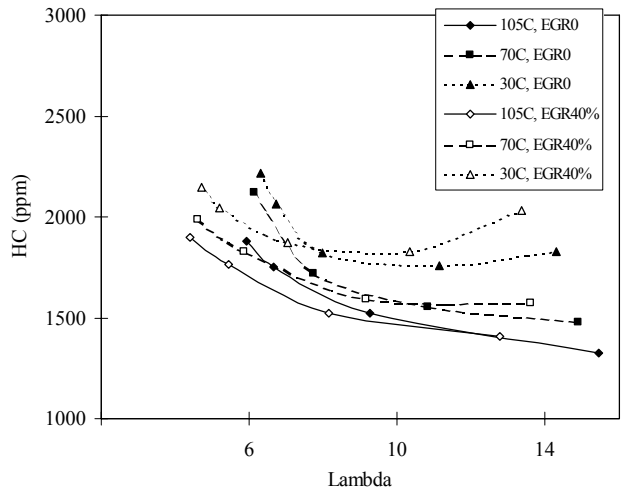

Figure 27 Effect of the intake temperature on HC emissions. (CR=18:1)

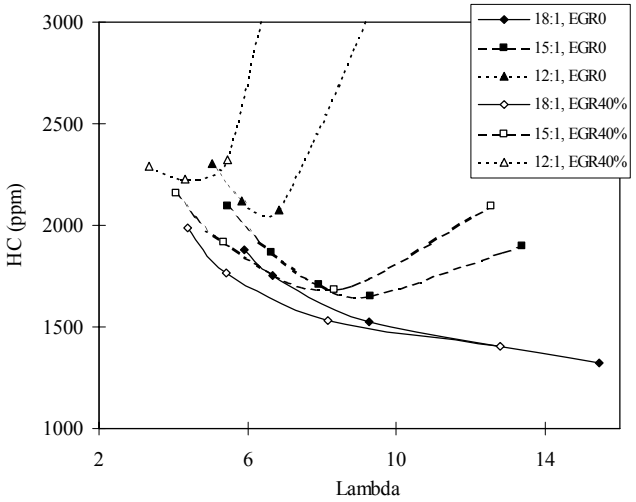

Figure 28 Effect of the compression ratio on HC emissions. (T_{in}=105°C)

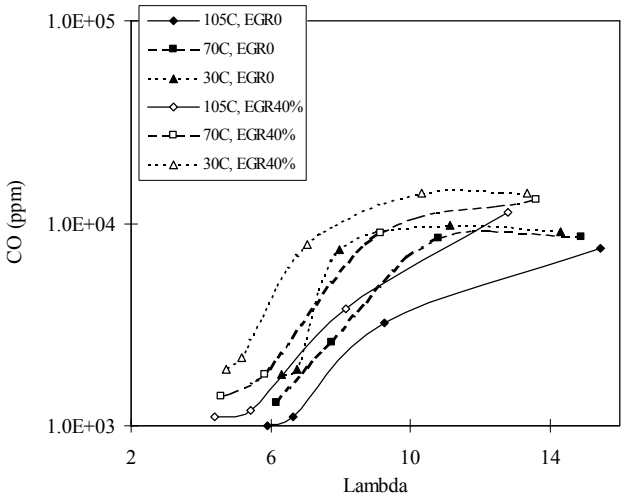

Figure 29 Effect of the intake temperature on CO emissions. (CR=18:1)

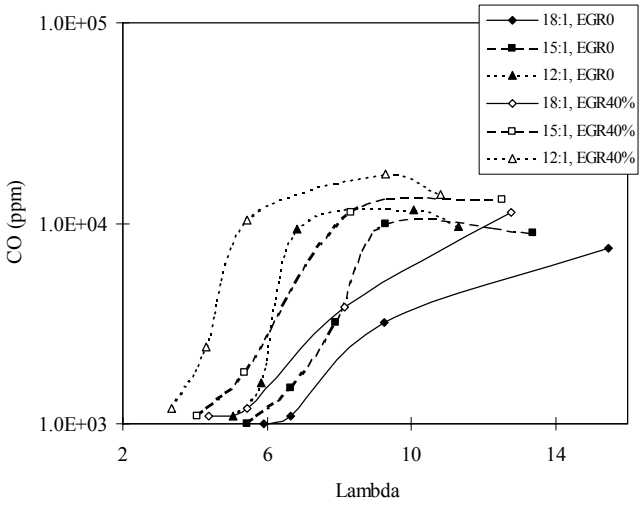

Figure 30 Effect of the compression ratio on CO emissions. (T_{in}=105°C)

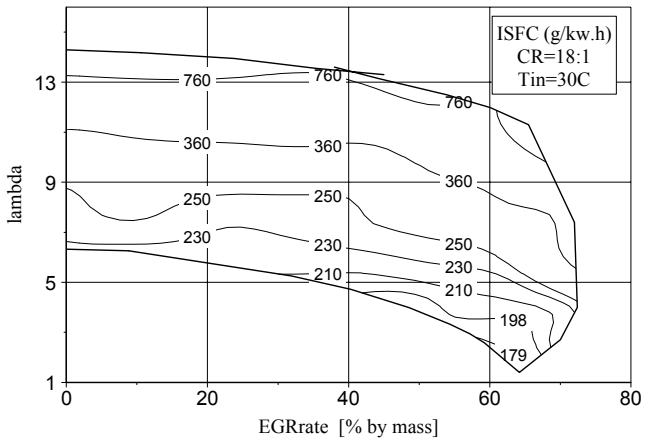

Figure 31 Effect of Air/Fuel ratio and EGR rate on ISFC. (CR=18:1 T_{in}=30°C)

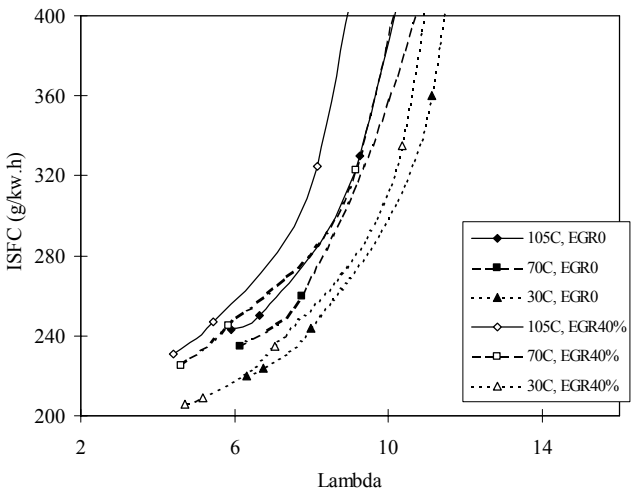

Figure 32 Effect of the intake temperature on ISFC. (CR=18:1)

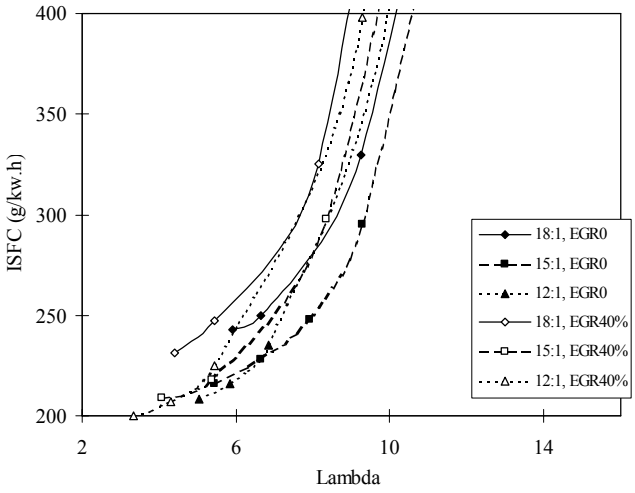

Figure 33 Effect of the compression ratio on ISFC. (CR=18:1)